Red-Emitting Tetracoordinate Organoboron Chelates: Synthesis, Photophysical Properties, and Fluorescence Microscopy

Vânia F. Pais,[†] Pedro Ramírez-López,[‡] Antonio Romero-Arenas,[‡] Daniel Collado,[§,⊥] Francisco Nájera,[§,⊥] Ezequiel Pérez-Inestrosa,[§,⊥] Rosario Fernández,[‖] José M. Lassaletta,[‡] Abel Ros,*[,‡,‖] and Uwe Pischel*[,†]

[†]CIQSO, Center for Research in Sustainable Chemistry and Department of Chemistry, University of Huelva, Campus de El Carmen s/n, 21071 Huelva, Spain

[‡]Institute for Chemical Research (CSIC-US) and Innovation-Center in Advanced Chemistry (ORFEO−CINQA), C/Américo Vespucio 49, 41092 Seville, Spain

[§]Department of Organic Chemistry, University of Málaga, IBIMA, Campus Teatinos s/n, 29071 Málaga, Spain

[⊥]Andalusian Center for Nanomedicine and Biotechnology, BIONAND, Parque Tecnológico de Andalucía, 29590 Málaga, Spain

[‖]Department of Organic Chemistry, University of Seville, and Innovation Center in Advanced Chemistry (ORFEO-CINQA), C/Prof. García González 1, 41012 Seville, Spain

Ⓢ *Supporting Information*

ABSTRACT: Seven tetracoordinate organoboron fluorophores with heterobiaryl N,O- or N,N-chelate ligands were prepared and photophysically characterized (in toluene). The electronic variation of the heteroaromatic moiety provided a means for the fine-tuning of the UV/vis absorption and emission spectra. In the most interesting cases, the spectra were red-shifted to maximum absorbance at wavelengths longer than 500 nm and emission maxima between 620 and 660 nm. The pronounced intramolecular charge-transfer character of the dyes yielded large Stokes shifts ($3500-5100$ cm^{-1}), while maintaining appreciable fluorescence quantum yields of up to 0.2 for emission maxima longer than 600 nm. The lipophilic character of the dyes enabled their application as stains of vesicle substructures in confocal fluorescence microscopy imaging.
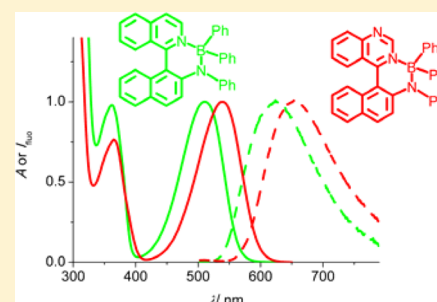
INTRODUCTION

The molecular design of fluorescent organoboron architectures has received renewed interest from their demonstrated utility in optoelectronic applications,[1−3] as sensors and switches,[4−7] or in bioimaging.[8−10] In particular, tetracoordinate boron(III) compounds with bidentate chelating ligands have been in the focus of these efforts.[11−15] The coordinative saturation of the boron center confers increased chemical stability and rigidity, often accompanied by significantly high fluorescence quantum yields. Excellent examples of boron(III) dyes with widespread application in chemical biology and sensing are Bodipy dyes.[4,8,16−21] The fluorescence emission of these compounds can be fine-tuned by manipulation of the substitution pattern, extension of the π-conjugate system, or heteroatom substitution in the chromophore skeleton, among other strategies.[22] Examples for such designs are electron-donor-substituted styryl Bodipy dyes[23] and aza-Bodipy dyes.[24−26] Modifications of the chromophore skeleton also have been proven to lead to pronounced red shifts of the emission in the case of xanthene dyes, for example sila or carbo derivatives of fluoresceins or rhodamines.[27−29] The extension of the π-conjugation of the chromophore, such as in naphthofluoresceins[30] or cyanine dyes,[31,32] is an often applied recipe for achieving emission in the red or even near-infrared (NIR) spectral region.[9] Fluorophores with red-shifted absorption and emission spectra are of particular interest in bioimaging because problems with the penetration depth of excitation light and reabsorption of emitted light by the biological tissue are widely avoided.[33−35]

In a recent work, we demonstrated the usefulness of arylisoquinoline-derived N,C ligands for the design of highly fluorescent compounds with applications in bioimaging (see Scheme 1).[10] The photophysical characteristics of these compounds are dominated by intramolecular charge-transfer (ICT) phenomena, providing large Stokes shifts and emissions that can be fine-tuned by electron-donor substitution and/or solvent effects. However, the most red-shifted emission of these fluorophores was still shorter than 600 nm. The desire to force the emission further toward the red spectral region triggered our efforts to synthesize related organoboron fluorophores with an arylisoquinoline skeleton or related N-heterocyclic ligands (see Chart 1), for example quinazolines. Interestingly, the latter have been integrated previously in push−pull architectures with interesting emission properties.[36,37]

Additional O- or N-electron-donor substituents were integrated with the expectation of achieving energetically lower-lying emissive states. Thereby the above outlined strategies of electronic manipulations of the chromophore
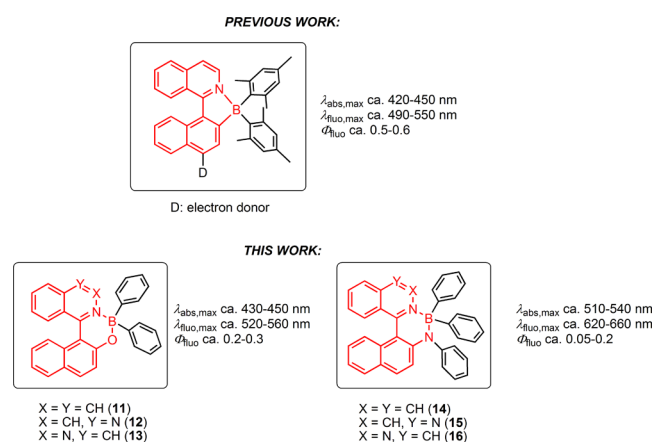
Scheme 1. Synthesis of Dyes 11−17
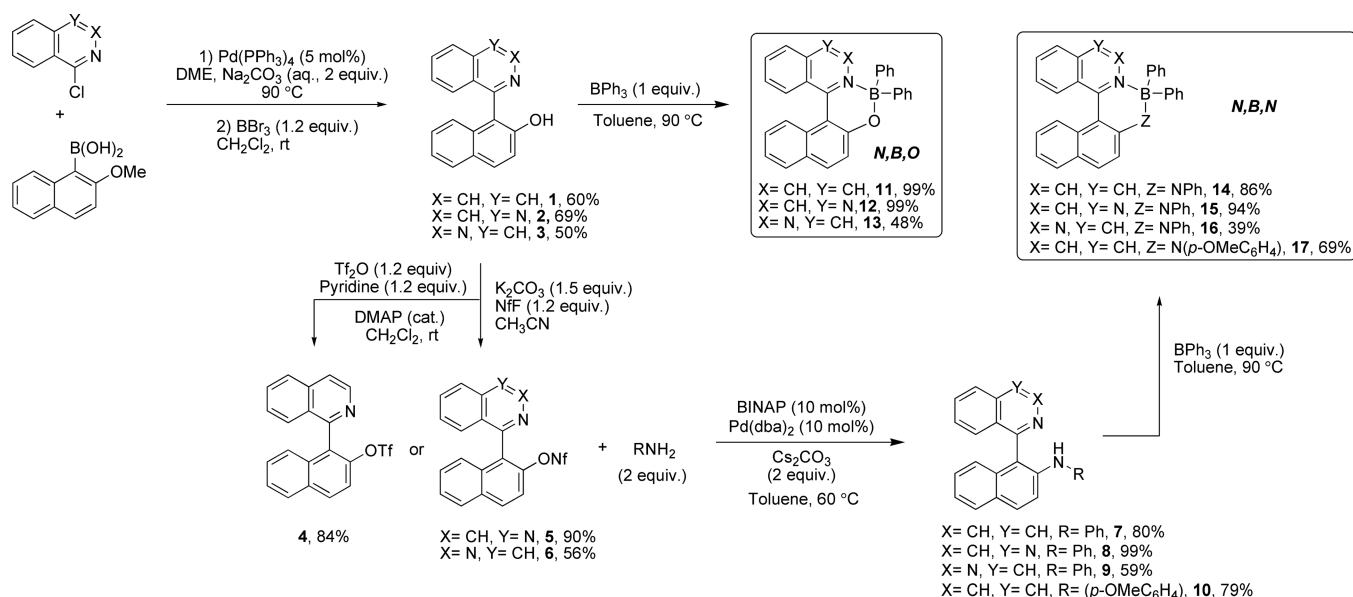
Chart 1. Structures and General Photophysical Properties of Azaaromatic-Based Organoboron Chelates

a All photophysical data refer to air-equilibrated toluene as solvent.

skeleton and its substitution pattern were synergistically combined. Interestingly, pronounced red shifts of the absorption and fluorescence spectra were obtained for some of the prepared dyes, while maintaining appreciable emission quantum yields of up to 0.2. The implication of ICT processes in the design of red-emitting fluorophores guarantees the desired large Stokes shifts but, unfortunately, often leads to very low emission quantum yields. This is a direct consequence of the energy gap law, favoring nonradiative deactivation of energetically low-lying emissive states, and may also be at least a partial explanation for efficient intersystem crossing to close-lying triplet states. With this in mind, the quantum yields reported herein are very significant.

Finally, the hydrophobic nature and structural shape of these fluorophores led to the prediction of a preferential accumulation in nonpolar cell compartments such as vesicle substructures,[38] which indeed was verified by confocal fluorescence microscopy imaging.

RESULTS AND DISCUSSION

Synthesis of the Organoboron Dyes 11−17. The synthesis of the N,B,O-dyes **11−13** was carried out with the corresponding known alcohols **1−3**,[39−41] by reaction with BPh$_3$ in anhydrous toluene at 90 °C (Scheme 1). After being heated overnight, the purification by conventional flash chromatography or precipitation afforded dyes **11−13** in moderate to excellent yields (48−99%). A similar strategy was employed for the synthesis of the N,B,N-dyes **14−17**, where the starting amines **7−10** were accessible by a Buchwald−Hartwig coupling reaction[42,43] between the triflate **4**[44] or the nonaflates **5** and **6**[41] and the corresponding aniline. Dyes **14−17** were obtained in moderate to excellent yields of 39−94% (see Supporting Information for more details). The identity and purity of the dyes was established by ^{1}H, ^{13}C, and ^{11}B NMR spectroscopy, as well as electrospray ionization high-resolution mass spectrometry, and elemental analysis.

Photophysical Properties. The UV/vis absorption and fluorescence properties of toluene solutions of the dyes prepared herein are summarized in Table 1, and representative spectra are shown in Figure 1. The absorption spectral properties show a clear dependence on the heterobiaryl skeleton (arylisoquinolines **11**, **14**; arylquinazolines **12**, **15**; arylphthalazines **13**, **16**) for both the N,B,O- and the N,B,N-

Table 1. Photophysical Properties of N,B,O-Dyes 11−13 and N,B,N-Dyes 14−17 in Air-Equilibrated Toluene Solution

	$\lambda_{\text{abs,max}}$ (nm)^a [ε (M^{-1} cm^{-1})]^b	$\lambda_{\text{fluo,max}}$ (nm)^c	Stokes shift (cm^{-1})	$\Phi_{\text{fluo}}{}^d$	τ_{fluo} (ns)^e
11	427 [5000]	522	4481	0.32	9.47
12	451 [5100]	543	3950	0.25	9.59
13	436 [3400]	555	5141	0.15	9.32
14	511 [6300]	623	3777	0.17	6.31
15	539 [8600]	654	3510	0.03	1.56
16	524 [2900]	657	4081	0.05	2.56
17	520 [6700]	641	3978	<0.01	0.25

a Absorption maximum. *b* Molar absorption coefficient. *c* Fluorescence maximum. *d* Fluorescence quantum yield. *e* Fluorescence lifetime.
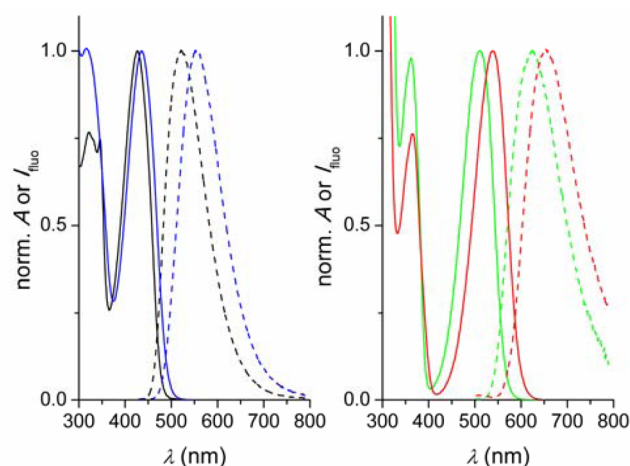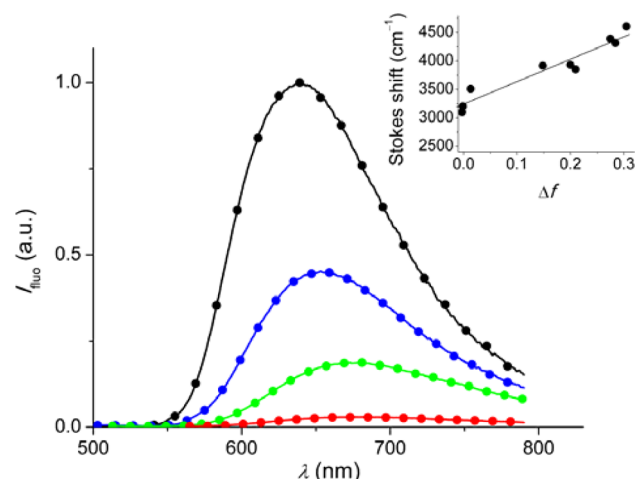
Figure 1. Normalized UV/vis absorption spectra (solid lines) and fluorescence spectra (dashed lines) of compounds **11** (black), **13** (blue), **14** (green), and **15** (red) in air-equilibrated toluene.

Figure 2. Fluorescence spectra of dye **15** in *n*-hexane (black), toluene (blue), chloroform (green), and *N,N*-dimethylformamide (red). The spectra are normalized to show the relative emission quantum yields in the different solvents. The inset shows the Lippert−Mataga plot ($n = 9$, $r^2 = 0.9151$) for dye **15**; see text.

dye series. In each series, the arylquinazoline dyes show the most red-shifted long-wavelength absorption maximum. Furthermore, generally the N,B,N-dyes have absorption (longer than 500 nm) and emission maxima more red-shifted than the N,B,O-dyes, extending to the red emission color. The dyes show increased Stokes shifts, varying between 3500 and 5100 cm^{-1}. The fluorescence quantum yields (Φ_{fluo}) follow clearly the energy gap law in photochemistry: nonradiative deactivation pathways become more competitive for energetically lower-lying emissive states. Hence, the fluorescence quantum yields drop for the N,B,N-dyes, although maintaining still quite appreciable levels considering that these dyes feature emission maxima longer than 600 nm (e.g., $\Phi_{fluo} = 0.17$ for dye **14**). The introduction of additional electron-donor substitution (i.e., a methoxy group in dye **17**) shifts the absorption and fluorescence maxima somewhat further to the red but mainly leads to a very accentuated drop of the emission quantum yield, again a direct consequence of the energy gap law. The fluorescence lifetimes (τ_{fluo}) were measured to be around 9.5 ns for the N,B,O-dyes and are more variable (0.25−6.31 ns) for the N,B,N-dyes.

In order to obtain further insights into the nature of the observed fluorescence, the solvent effect was studied for selected N,B,N-dyes. Note that the N,B,O-dyes show insufficient chemical stability in solvents such as tetrahydrofuran, *N,N*-dimethylformamide, and sometimes in acetonitrile. The N,B,N-dyes show a hypsochromic shift of the UV/vis absorption spectrum (negative solvatochromism) when changing from nonpolar toluene to polar acetonitrile, whereas the emission bands shift bathochromically (positive solvatochromism). As a result, the Stokes shift is increased in acetonitrile. This effect is most accentuated for dyes **15** and **16** for which notable Stokes shifts of 4600 and 5100 cm^{-1}, respectively, were observed. However, expectedly, this comes at the expense of a drastically reduced emission quantum yield for these two dyes, being lower than 0.01 in acetonitrile. In order to establish a more detailed trend, a series of nine solvents, addressing aspects such as polarity, hydrogen bonding character, and viscosity, were studied for dye **15** (Figure 2 and detailed data in Supporting Information).

Beside the above-mentioned positive solvatochromism of the emission spectrum, the following general trends can be derived:

(a) protic solvents deactivate the fluorescence practically totally ($\Phi_{fluo} < 10^{-3}$ in methanol); (b) in nonpolar solvents, the highest fluorescence quantum yields are observed ($\lambda_{fluo,max} = 641$ nm, $\Phi_{fluo} = 0.06$ in *n*-hexane); (c) increasing viscosity has no influence on the fluorescence ($\lambda_{fluo,max} = 642$ nm, $\Phi_{fluo} = 0.07$ in decalin). Treatment of the data according to the Lippert−Mataga equation[45−47] yielded a dipole moment change ($\Delta\mu$) between the ground and the excited state of 10 D. This suggests an accentuated ICT character of the emissive state and is in line with our recent results on N,C-chelate tetracoordinate arylisoquinoline organoboron compounds.[10] The ICT character explains the observed large Stokes shifts (see above).

The occurrence of ICT was confirmed by time-dependent density functional theory calculations[48] (CAM-B3LYP/6-311+G(2d,p) level of theory) of **11**, **14**, **15**, and **16** as representative dyes (see Supporting Information). The lowest-energy emission ($S_1 \rightarrow S_0$) corresponds mainly to a LUMO → HOMO transition (contribution of 95−97%). The contour plots of the frontier orbitals show that the HOMO is mainly located on the naphthyl-derived "half" of the system, while the LUMO has its main contribution from the heteroaromatic moiety; see Figure 3 for the examples of dyes **11** and **15**. The
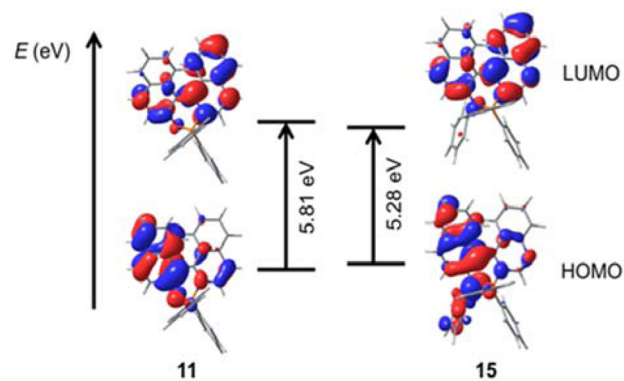

Figure 3. HOMO/LUMO isosurface plots and frontier orbital energies of dyes **11** and **15**.

natural transition orbital analysis yielded the same conclusion of an effective ICT process on excitation of the dyes. This observation resembles similar results that were obtained for related borylated arylisoquinoline dyes.[10,49]

Bioimaging Applications. The negligible fluorescence in protic media as contrasted by the significant fluorescence in nonpolar environments prompted us to investigate the use of the lipophilic organoboron N,N-chelates as probes for cellular lipid substructures such as vesicles.[38,50,51] For this purpose, dyes **15** and **16** were incubated with N13 mouse microglial cells. In a first approach, cell viability studies were performed by applying a flow cytometry method using simultaneously Hoechst 33342 and propidium iodide staining.[52] This yielded a cell viability of 83% following 24 h of incubation for both dyes at a concentration of 10 μM. These data were confirmed by high-throughput screening with automated microscopy using the same nuclear stains: 86% viability for **15** and 88% for **16** after 24 h incubation.

In Figure 4, images of N13 cells stained with dye **15**, Hoechst 33342 as a marker of the cell nucleus, and Atto488-conjugated
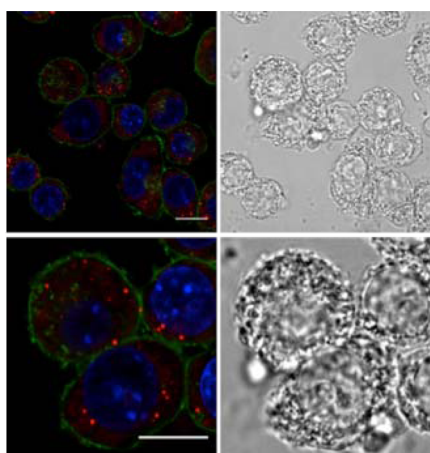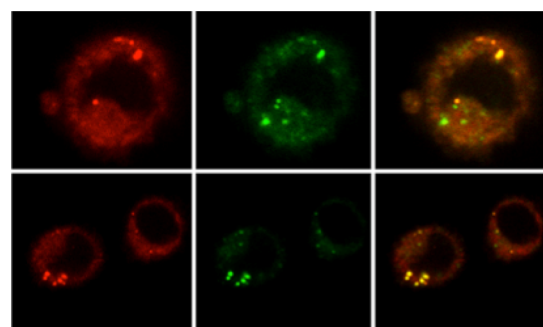

Figure 4. Confocal fluorescence microscopy images (left) of N13 mouse microglial cells incubated (for 24 h) with dye **15** (10 μM) (red). The submembrane actin (green) was stained with Atto488-conjugated phalloidin (0.1 μM) and the nucleus (blue) with Hoechst 33342 (8 μM). Transmission microscopy images are shown on the right side. Scale bars: 10 μm.

phalloidin as a marker for submembrane actin are shown. For many organic fluorophores, a homogeneous cytoplasmic accumulation is typical, while for our dyes, just a very weak "cloud-like" fluorescence was evident. This is in accordance with the strongly deactivated fluorescence of the dye in polar (protic) media. However, a clear light-up behavior for the dye accumulation in some small intracellular substructures was observed. With the considerably higher fluorescence in nonpolar environments in mind, we interpreted this as the accumulation in vesicle-like substructures. Colocalization imaging (Figure 5) demonstrated the specific accumulation of the investigated dyes **15** and **16** in structures that are also marked by the liphophilic styryl dye FM4-64.[53]

CONCLUSIONS

In summary, lipophilic tetracoordinate N,O- and N,N-chelate organoboron dyes show distinct photophysical properties that enable their application as vesicle stains in confocal fluorescence microscopy imaging. On the one hand, the N,O-

Figure 5. Confocal fluorescence microscopy images of N13 mouse microglial cells. On the left, the labeling with dye **15** (top row) and **16** (bottom row), both at 30 μM, is shown. The middle images show the corresponding labeling with the lipophilic probe FM4-64, and the overlay is shown on the right.

chelates show green-to-yellow emission with quantum yields of up to 0.3 in toluene. On the other hand, the N,N-chelates are characterized by fluorescence emission maxima longer than 600 nm, maintaining significant fluorescence quantum yields (up to 0.2 in toluene). The emission quantum yields in the N,B,N series are generally lower than that in the N,B,O series, which is a direct consequence of the energy gap law and more dominant nonradiative deactivation pathways. The large Stokes shifts of ca. 3500−5100 cm^{-1} (in toluene) that are typical for the verified intramolecular charge-transfer phenomena and the pronounced solvent dependence of the emission (especially of the N,B,N-dyes) are additional attributes of the functional characteristics.

EXPERIMENTAL SECTION

General Methods. ^{1}H NMR spectra were recorded at 400 or 500 MHz; ^{13}C NMR spectra were recorded at 100 or 125 MHz with the solvent peak used as the internal reference (7.26 and 77.0 ppm for ^{1}H and ^{13}C, respectively). ^{11}B NMR spectra were recorded with complete proton decoupling at 128 MHz and using BF$_3$·Et$_2$O (0.00 ppm for ^{11}B NMR) as an external standard. Electrospray ionization high-resolution mass spectra were obtained with a QTRAP mass spectrometer (hybrid triple-quadrupole/linear ion trap mass spectrometer). Column chromatography was performed on silica gel. Analytical TLC was performed on aluminum-backed plates (1.5 × 5 cm) precoated (0.25 mm) with silica gel. Compounds were visualized by exposure to UV light or by dipping the plates in a solution of 5% (NH$_4$)$_2$Mo$_7$O$_{24}$·4H$_2$O in 95% EtOH (w/v).

Anhydrous 1,4-dioxane and THF were obtained by distillation from sodium using benzophenone as an indicator. Pd(dba)$_2$, BPh$_3$, BINAP ligand, aniline, and p-anisidine were commercially available. The alcohols **1**−**3**,[39−41] the triflate **4**,[44] and the nonaflates **5** and **6**[41] are known compounds. The NMR spectra of the analogously prepared compounds herein were found to resemble the published data.

The solvents for the photophysical measurements were of spectroscopic quality and used as received.

General Procedure for the Synthesis of 7−10. A flamed-dried Schlenk tube was charged with the corresponding triflate **4** or nonaflates **5** and **6**. (0.2 mmol), Cs$_2$CO$_3$ (0.4 mmol, 130.2 mg), Pd(dba)$_2$ (10 mol %, 11.6 mg), and BINAP (10 mol %, 12.4 mg). After three cycles of vacuum argon flushing, deoxygenated dry toluene (4 mL) and the appropriate amine (0.4 mmol) were sequentially added in this order. The reaction mixture was stirred at 60 °C for 24 h, cooled to room temperature, and filtered through a Celite pad. The solvent was removed under vacuum, and the resulting residue was purified by column chromatography on silica gel.

Compound 7. Following the general procedure starting from **4**, purification by flash chromatography (CH$_2$Cl$_2$/EtOAc 50:1 → 10:1) gave **7** (55 mg, 80%) as a yellow foam: ^{1}H NMR (400 MHz, CDCl$_3$) δ

8.78 (d, 1H, J = 5.8 Hz), 7.93 (d, 1H, J = 8.3 Hz), 7.88 (d, 1H, J = 9.0 Hz), 7.83 (d, 1H, J = 8.0 Hz), 7.78 (dd, 1H, J = 5.7 and 0.6 Hz), 7.71 (d, 1H, J = 9.0 Hz), 7.68 (ddd, 1H, J = 8.2, 6.9, and 1.2 Hz), 7.60 (dd, 1H, J = 8.5 and 0.8 Hz), 7.39 (ddd, 1H, J = 8.4, 7.0, and 1.2 Hz), 7.30 (ddd, 1H, J = 8.1, 6.9, and 1.2 Hz), 7.23–7.16 (m, 3H), 7.02–6.97 (m, 2H), 6.95–6.91 (m, 1H), 6.88 (t, 1H, J = 7.3 Hz), 6.05 (s, 1H) ppm; ^{13}C NMR (100 MHz, CDCl$_3$) δ 158.6, 143.1, 142.9, 139.4, 136.9, 134.0, 130.7, 129.7, 129.4, 129.3, 128.6, 128.2, 127.8, 127.5, 127.2, 126.7, 124.9, 123.5, 121.9, 121.4, 120.7, 119.1, 118.8 ppm; HRMS (ESI) calcd C$_{25}$H$_{19}$N$_2$ for (M + H$^+$) 347.1543, found 347.1537. Anal. Calcd for C$_{25}$H$_{18}$N$_2$: C, 86.68; H, 5.24; N, 8.09. Found: C, 86.65; H, 5.26; N, 8.21.

Compound 8. Following the general procedure starting from **5**, purification by flash chromatography (*n*-hexane/EtOAc 3:1) gave **8** (69 mg, 99%) as a yellow foam: ^{1}H NMR (400 MHz, CDCl$_3$) δ 9.45 (s, 1H), 8.08 (d, 1H, J = 8.5 Hz), 7.91 (d, 1H, J = 9.0 Hz), 7.86 (ddd, 1H, J = 8.5, 6.9, and 1.4 Hz), 7.84 (d, 1H, J = 8.0 Hz), 7.71 (d, 1H, J = 9.1 Hz), 7.66–7.59 (m, 1H), 7.44 (ddd, 1H, J = 8.3, 7.0, and 1.1 Hz), 7.33 (ddd, 1H, J = 8.0, 6.9, and 1.1 Hz), 7.27–7.17 (m, 3H), 7.07–7.01 (m, 2H), 6.97 (d, 1H, J = 8.5 Hz), 6.92 (t, 1H, J = 1.0 Hz), 6.47 (br s, 1H) ppm; ^{13}C NMR (100 MHz, CDCl$_3$) δ 167.7, 155.1, 150.9, 142.3, 139.5, 134.4, 133.1, 130.6, 129.3, 129.1, 128.9, 128.2, 128.1, 127.1, 127.0, 125.0, 124.3, 123.8, 121.7, 119.2, 119.1, 118.9 ppm; HRMS (ESI) calcd for C$_{24}$H$_{18}$N$_3$ (M + H$^+$) 348.1495, found 348.1500. Anal. Calcd for C$_{24}$H$_{17}$N$_3$: C, 82.97; H, 4.93; N, 12.10. Found: C, 82.89; H, 5.21; N, 11.89.

Compound 9. Following the general procedure starting from **6**, purification by flash chromatography (*n*-hexane/EtOAc 3:1) gave **9** (41 mg, 59%) as a yellow amorphous solid: mp 224–226 °C; ^{1}H NMR (400 MHz, CDCl$_3$) δ 9.63 (s, 1H), 8.05 (d, 1H, J = 8.1 Hz), 7.95–7.86 (m, 2H), 7.85 (d, 1H, J = 8.1 Hz), 7.73 (d, 1H, J = 9.1 Hz), 7.69 (t, 1H, J = 7.3 Hz), 7.55 (d, 1H, J = 8.3 Hz), 7.32 (t, 1H, J = 7.3 Hz), 7.25–7.13 (m, 3H), 6.99 (d, 1H, J = 7.8 Hz), 6.93 (d, 1H, J = 8.5 Hz), 6.88 (t, 1H, J = 7.3 Hz), 6.37 (br s, 1H) ppm; ^{13}C NMR (100 MHz, CDCl$_3$) δ 158.7, 151.1, 142.5, 139.8, 133.7, 132.8, 130.3, 129.2, 128.1, 127.0, 126.9, 126.8, 126.6, 126.2, 124.5, 123.7, 121.4, 119.3, 118.6, 118.5 ppm; HRMS (ESI) calcd for C$_{24}$H$_{18}$N$_3$ (M + H$^+$) 348.1495, found 348.1491. Anal. Calcd for C$_{24}$H$_{17}$N$_3$: C, 82.97; H, 4.93; N, 12.10. Found: C, 82.61; H, 5.33; N, 11.71.

Compound 10. Following the general procedure starting from **4**, purification by flash chromatography (toluene/EtOAc 10:1) gave **10** (59 mg, 79%) as a light yellow foam: ^{1}H NMR (400 MHz, CDCl$_3$) δ 8.78 (d, 1H, J = 5.7 Hz), 7.94 (d, 1H, J = 8.3 Hz), 7.83 (d, 1H, J = 9.1 Hz), 7.80 (m, 2H), 7.70 (ddd, 1H, J = 8.0, 6.9, and 1.1 Hz), 7.64 (d, 1H, J = 8.3 Hz), 7.49 (d, 1H, J = 9.1 Hz), 7.42 (ddd, 1H, J = 8.2, 7.0, and 1.0 Hz), 7.28–7.22 (m, 1H), 7.18 (ddd, 1H, J = 8.2, 6.9, and 1.3 Hz), 7.03–6.95 (m, 2H), 6.88 (d, 1H, J = 8.4 Hz), 6.82–6.75 (m, 2H), 5.76 (br s, 1H), 3.75 (s, 3H) ppm; ^{13}C NMR (100 MHz, CDCl$_3$) δ 158.6, 155.6, 142.8, 141.4, 137.1, 135.7, 134.0, 131.0, 129.9, 128.7, 128.2, 127.9, 127.7, 127.2, 126.8, 124.5, 123.0, 120.8, 119.1, 117.8, 114.7, 55.7 ppm; HRMS (ESI) calcd for C$_{26}$H$_{21}$N$_2$O (M + H$^+$) 377.1648, found 377.1641. Anal. Calcd for C$_{26}$H$_{20}$N$_2$O: C, 82.95; H, 5.36; N, 7.44. Found: C, 82.98; H, 5.72; N, 7.29.

General Procedure for the Synthesis of 11–17. A dried Schlenk tube was charged with substrates **1–3** or **7–10** (0.1–0.2 mmol) and BPh$_3$ (1 equiv). After three cycles of vacuum argon flushing, 1 mL of dried deoxygenated toluene was added. The reaction mixture was stirred at 90 °C until reaching maximum consumption of the starting material (TLC monitoring), cooled to room temperature, and finally concentrated to dryness. The crude products were purified by column chromatography on silica gel (*n*-hexane/EtOAc, toluene/EtOAc, or CH$_2$Cl$_2$/EtOAc mixtures as eluents) or by being washed with *n*-hexane/EtOAc mixtures.

Compound 11. Following the general procedure starting from **1** (0.1 mmol, 27 mg) and heating for 18 h, flash chromatography on silica gel (*n*-hexane/EtOAc 1:3) gave **11** (43 mg, 99%) as a yellow foam: ^{1}H NMR (400 MHz, CDCl$_3$) δ 8.05 (d, 1H, J = 5.6 Hz), 7.94–7.88 (m, 3H), 7.83 (t, 1H, J = 7.8 Hz), 7.73 (d, 1H, J = 8.8 Hz), 7.65 (d, 1H, J = 6.6 Hz), 7.48 (d, 1H, J = 8.8 Hz), 7.45 (t, 1H, J = 8.2 Hz), 7.39–7.37 (m, 2H), 7.32–7.25 (m, 7H), 7.14 (ddd, 1H, J = 8.6, 6.6,

and 1.2 Hz), 7.04 (t, 2H, J = 7.0 Hz), 6.97 (t, 1H, J = 7.0 Hz) ppm; ^{13}C NMR (100 MHz, CDCl$_3$) δ 163.4, 151.5, 137.6, 136.1, 134.9, 134.4, 132.9, 132.3, 131.9, 131.0, 128.5, 128.4, 127.7, 127.6, 127.0, 126.9, 126.7, 126.1, 125.5, 125.1, 124.7, 123.3, 121.7, 119.6, 113.8 ppm (C–B not observed); ^{11}B NMR (128 MHz, CDCl$_3$) δ 6.1 (br s) ppm; HRMS (ESI) calcd for C$_{31}$H$_{23}$BNO (M + H$^+$) 436.1867, found 436.1847.

Compound 12. Following the general procedure starting from **2** (0.2 mmol, 54 mg) and heating for 20 h, the reaction crude was triturated with a *n*-hexane/EtOAc 3:1 mixture to give **12** (88 mg, 99%) as a yellow-orange foam: ^{1}H NMR (400 MHz, CDCl$_3$) δ 8.82 (s, 1H), 8.11 (d, 1H, J = 8.2 Hz), 7.99 (ddd, 1H, J = 8.2, 6.9, and 1.2 Hz), 7.97 (d, 1H, J = 9.0 Hz), 7.93 (d, 1H, J = 8.6 Hz), 7.74 (d, 1H, J = 7.6 Hz), 7.49 (ddd, 1H, J = 8.2, 7.0, and 1.1 Hz), 7.46 (d, 1H, J = 8.9 Hz), 7.42–7.38 (m, 3H), 7.34–7.29 (m, 4H), 7.24–7.21 (m, 3H), 7.08 (t, 2H, J = 7.0 Hz), 7.02 (t, 1H, J = 7.2 Hz) ppm; ^{13}C NMR (100 MHz, CDCl$_3$) δ 165.8, 155.9, 150.6, 147.9, 137.7, 136.2, 134.3, 132.1, 131.8, 130.1, 128.9, 128.7, 128.6, 128.1, 127.8, 127.4, 126.9, 125.9, 124.7, 124.3, 121.8, 119.8, 112.5 ppm (C–B not observed); ^{11}B NMR (128 MHz, CDCl$_3$) δ 5.5 (br s) ppm; HRMS (ESI) calcd for C$_{30}$H$_{22}$BN$_2$O (M + H$^+$) 437.1820, found 437.1799.

Compound 13. Following the general procedure starting from **3** (0.2 mmol, 54 mg) and heating for 48 h, starting material still remained. Flash chromatography on silica gel (*n*-hexane/EtOAc 2:1 → 1:1) gave **13** (40 mg, 48%) as a yellow foam: ^{1}H NMR (400 MHz, CDCl$_3$) δ 9.30 (s, 1H), 8.07–8.03 (m, 2H), 7.99 (d, 1H, J = 9.0 Hz), 7.96 (d, 1H, J = 8.9 Hz), 7.78–7.74 (m, 2H), 7.54 (d, 1H, J = 8.9 Hz), 7.44 (d, 2H, J = 6.7 Hz), 7.36 (d, 2H, J = 6.2 Hz), 7.30–7.21 (m, 5H), 7.16 (ddd, 1H, J = 8.2, 6.8, and 1.2 Hz), 7.08 (t, 2H, J = 7.4 Hz), 7.01 (t, 1H, J = 7.2 Hz) ppm; ^{13}C NMR (100 MHz, CDCl$_3$) δ 164.2, 151.1, 148.4, 136.3, 134.7, 133.9, 132.5, 132.4, 131.6, 130.0, 128.8, 128.6, 127.5, 127.0, 126.8, 126.7, 126.5, 125.7, 125.6, 124.2, 123.7, 122.0, 110.8 ppm (C–B not observed); ^{11}B NMR (128 MHz, CDCl$_3$) δ 6.1 (br s) ppm; HRMS (ESI) calcd for C$_{30}$H$_{22}$BN$_2$O (M + H$^+$) 437.1820, found 437.1801.

Compound 14. Following the general procedure starting from **7** (0.1 mmol, 34.6 mg) and heating for 7 h, flash chromatography on silica gel (*n*-hexane/EtOAc 3:1) gave **14** (44 mg, 86%) as a deep red foam: ^{1}H NMR (400 MHz, CDCl$_3$) δ 8.00 (d, 1H, J = 6.7 Hz), 7.92 (d, 1H, J = 8.6 Hz), 7.87 (d, 1H, J = 8.0 Hz), 7.75 (t, 1H, J = 7.8 Hz), 7.63 (d, 1H, J = 9.2 Hz), 7.61 (d, 1H, J = 8.0 Hz), 7.52 (d, 1H, J = 6.7 Hz), 7.38 (ddd, 1H, J = 8.3 6.9 and 1.0 Hz), 7.32 (d, 1H, J = 9.2 Hz), 7.28–7.26 (m, 2H), 7.20–7.15 (m, 4H), 7.13 (ddd, 1H, J = 7.9, 6.9, and 1.2 Hz), 7.08–6.91 (m, 9H), 6.81–6.80 (m, 2H) ppm; ^{13}C NMR (100 MHz, CDCl$_3$) δ 153.4, 151.2, 147.5, 136.9, 136.3, 133.3, 133.1, 132.7, 132.1, 131.4, 129.2, 128.0, 127.9, 127.3, 126.8, 126.6, 126.0, 125.5, 125.1, 125.0, 123.0, 122.6, 121.1, 117.9, 113.2 ppm (C–B not observed); ^{11}B NMR (128 MHz, CDCl$_3$) δ 3.8 (br s) ppm; HRMS (ESI) calcd for C$_{37}$H$_{28}$BN$_2$ (M + H$^+$) 511.2340, found 511.2325. Anal. Calcd for C$_{37}$H$_{27}$BN$_2$: C, 87.06; H, 5.33; N, 5.49. Found: C, 87.09; H, 5.82; N, 5.23.

Compound 15. Following the general procedure starting from **8** (0.1 mmol, 34.7 mg) and heating for 12 h, flash chromatography on silica gel (toluene) gave **15** (48 mg, 94%) as a purple foam: ^{1}H NMR (400 MHz, CDCl$_3$) δ 8.75 (s, 1H), 8.00 (d, 1H, J = 8.0 Hz), 7.89 (d, 1H, J = 8.5 Hz), 7.85 (ddd, 1H, J = 8.3, 7.0, and 1.2 Hz), 7.65 (d, 1H, J = 9.3 Hz), 7.61 (d, 1H, J = 7.9 Hz), 7.37 (ddd, 1H, J = 8.3, 7.1, and 1.1 Hz), 7.29–7.17 (m, 8H), 7.09–6.93 (m, 9H), 6.90–6.88 (m, 2H) ppm; ^{13}C NMR (100 MHz, CDCl$_3$) δ 155.1, 153.5, 149.2, 147.9, 146.3, 135.4, 134.7, 133.1, 133.0, 130.2, 129.2, 128.5, 128.2, 128.1, 127.5, 127.4, 127.0, 126.8, 126.7, 126.4, 125.4, 125.3, 124.3, 123.8, 120.6, 120.2, 111.3 ppm (C–B not observed); ^{11}B NMR (128 MHz, CDCl$_3$) δ 2.9 (br s) ppm; HRMS (ESI) calcd for C$_{36}$H$_{27}$N$_3$ (M + H$^+$) 512.2293, found 512.2276. Anal. Calcd for C$_{36}$H$_{26}$BN$_3$: C, 84.55; H, 5.12; N, 8.22. Found: C, 84.42; H, 5.20; N, 8.25.

Compound 16. Following the general procedure starting from **9** (0.1 mmol, 34.7 mg), and heating for 72 h, starting material still remained. Flash chromatography on silica gel (*n*-hexane/EtOAc 3:1) gave **16** (20 mg, 39%) as a purple foam: ^{1}H NMR (400 MHz, CDCl$_3$) δ 9.16 (d, 1H, J = 0.8 Hz), 7.99 (d, 1H, J = 8.2 Hz), 7.98 (dd, 1H, J =

7.5 and 1.4 Hz), 7.92 (ddd, 1H, J = 8.0, 7.0, and 1.0 Hz), 7.69−7.63 (m, 3H), 7.46−7.44 (m, 2H), 7.29 (d, 1H, J = 9.2 Hz), 7.17 (ddd, 1H, J = 8.0, 6.8, and 1.2 Hz), 7.10−7.05 (m, 4H), 7.03−6.91 (m, 11H) ppm; ^{13}C NMR (100 MHz, CDCl$_3$) δ 153.9, 148.8, 147.1, 147.0, 135.9, 133.9, 133.6, 133.4, 132.8, 132.0, 130.2, 128.2, 128.0, 127.5, 127.2, 126.6, 126.4, 126.3, 126.2, 125.3, 125.2, 124.6, 123.6, 123.1, 121.1, 109.3 ppm (C−B not observed); ^{11}B NMR (128 MHz, CDCl$_3$) δ 4.0 (br s) ppm; HRMS (ESI) calcd for C$_{36}$H$_{26}$BN$_3$Na (M + Na$^+$) 534.2112, found 534.2102.

Compound 17. Following the general procedure starting from **10** (0.1 mmol, 37.6 mg) and heating for 12 h, flash chromatography on silica gel (*n*-hexane/CH$_2$Cl$_2$ 1:3) gave **17** (37 mg, 69%) as a purple foam: ^{1}H NMR (400 MHz, CDCl$_3$) δ 7.98 (d, 1H, J = 6.7 Hz), 7.91 (d, 1H, J = 8.7 Hz), 7.86 (d, 1H, J = 8.1 Hz), 7.73 (t, 1H, J = 7.9 Hz), 7.62 (d, 1H, J = 9.2 Hz), 7.60 (d, 1H, J = 7.8 Hz), 7.50 (d, 1H, J = 6.7 Hz), 7.36 (t, 1H, J = 8.1 Hz), 7.28−7.24 (m, 3H), 7.13−6.93 (m, 12H), 6.75 (d, 2H, J = 8.8 Hz), 6.48 (dd, 1H, J = 8.8 and 2.8 Hz), 3.72 (s, 3H) ppm; ^{13}C NMR (100 MHz, CDCl$_3$) δ 155.6, 153.7, 151.0, 140.8, 136.9, 136.2, 133.4, 133.2, 132.7, 132.0, 131.4, 129.9, 128.2, 127.9, 127.2, 127.1, 126.8, 126.6, 126.0, 125.9, 125.4, 125.1, 125.0, 122.5, 121.0, 117.7, 113.7, 112.9, 112.6, 55.3 ppm (C−B not observed); ^{11}B NMR (128 MHz, CDCl$_3$) δ 3.7 (br s) ppm; HRMS (ESI) calcd for C$_{38}$H$_{30}$BN$_2$O (M + H$^+$) 541.2446, found 541.2435. Anal. Calcd for C$_{38}$H$_{29}$BN$_2$O: C, 84.45; H, 5.41; N, 5.18. Found: C, 84.56; H, 5.33; N, 5.02.

Photophysical Measurements. The photophysical data were obtained for air-equilibrated solutions at room temperature. The UV/vis absorption spectra and the fluorescence spectra were recorded with standard instrumentation. The emission spectra were corrected for the sensitivity of the photomultiplier detector. The fluorescence quantum yields were determined with 4-amino-*N*-propyl-1,8-naphthalimide (Φ_{fluo} = 0.48 in acetonitrile)[38] or tris(2,2′-bipyridyl)dichloro-ruthenium(II) hexahydrate (Φ_{fluo} = 0.028 in air-equilibrated water)[54] as reference and corrected for refractive index differences of the used solvents. The lifetime measurements were performed by means of time-correlated single-photon counting with a picosecond pulsed diode laser (λ = 442 nm, pulse width fwhm 78 ps, λ = 482 nm, pulse width fwhm 101 ps) as excitation sources.

Confocal Fluorescence Microscopy. N13 mouse microglia cells were grown to 60% confluence on 8-well slides in complete medium (CM) containing Roswell Park Memorial Institute 1640 medium supplemented with 10% fetal calf serum, penicillin (100 units mL^{-1}), streptomycin (100 μg mL^{-1}), and gentamicin (1.25 units mL^{-1}). Organoboron dyes were diluted in fresh CM, added to each well, and cultured under optimal conditions (37 °C and 5% CO$_2$ in a humidified incubator) for a further 24 h. Live cells were examined using a microscope stage-top incubator to maintain cells under optimal conditions (37 °C, 5% CO$_2$, and humidity) during imaging. Co-staining, using the lipophilic marker FM4-64FX, was achieved by adding it directly to the culture medium at a 5 μg mL^{-1} final concentration. For fixation, cells were washed with prewarmed phosphate buffer saline (PBS), incubated with 4% paraformaldehyde in PBS for 20 min at room temperature, and washed three times with PBS. Submembrane actin and nuclei (DNA) were labeled for 20 min with 0.1 μM Atto488-conjugated phalloidin and 8 μM Hoechst 33342, respectively. Live and fixed cells were analyzed using an inverted microscope, a 25× NA 0.95 Plan-APO water immersion objective, and a laser scanning confocal system. In live cells, the emission of the organoboron dyes and FM4-64FX was detected using 561 and 594 nm excitation wavelengths with 569−635 and 712−774 nm detection windows, respectively. In fixed cells, Hoechst 33258, Atto488 phalloidin, and the organoboron dyes were detected using 405, 488, and 561 nm excitation wavelengths with 415−470, 493−555, and 668−690 nm detection windows, respectively. Channels were acquired sequentially and configured to avoid crosstalk between different fluorophores.

■ ASSOCIATED CONTENT

⑤ Supporting Information

The Supporting Information is available free of charge on the ACS Publications website at DOI: 10.1021/acs.joc.6b01569.

Copies of ^{1}H and ^{13}C NMR spectra, details of the DFT calculations, and additional photophysical data (PDF)

■ AUTHOR INFORMATION

Corresponding Authors
*E-mail abel.ros@iiq.csic.es.
*E-mail uwe.pischel@diq.uhu.es.

Notes

The authors declare no competing financial interest.

■ ACKNOWLEDGMENTS

■ REFERENCES

(1) Wakamiya, A.; Taniguchi, T.; Yamaguchi, S. *Angew. Chem., Int. Ed.* **2006**, *45*, 3170−3173.

(2) Entwistle, C. D.; Marder, T. B. *Angew. Chem., Int. Ed.* **2002**, *41*, 2927−2931.

(3) Rao, Y.-L.; Wang, S. *Inorg. Chem.* **2011**, *50*, 12263−12274.

(4) Bozdemir, O. A.; Guliyev, R.; Buyukcakir, O.; Selcuk, S.; Kolemen, S.; Gulseren, G.; Nalbantoglu, T.; Boyaci, H.; Akkaya, E. U. *J. Am. Chem. Soc.* **2010**, *132*, 8029−8036.

(5) Kowada, T.; Maeda, H.; Kikuchi, K. *Chem. Soc. Rev.* **2015**, *44*, 4953−4972.

(6) Rao, Y.-L.; Amarne, H.; Zhao, S.-B.; McCormick, T. M.; Martić, S.; Sun, Y.; Wang, R.-Y.; Wang, S. *J. Am. Chem. Soc.* **2008**, *130*, 12898−12900.

(7) Baik, C.; Hudson, Z. M.; Amarne, H.; Wang, S. *J. Am. Chem. Soc.* **2009**, *131*, 14549−14559.

(8) Kolemen, S.; Işık, M.; Kim, G. M.; Kim, D.; Geng, H.; Buyuktemiz, M.; Karatas, T.; Zhang, X.-F.; Dede, Y.; Yoon, J.; Akkaya, E. U. *Angew. Chem., Int. Ed.* **2015**, *54*, 5340−5344.

(9) Lavis, L. D.; Raines, R. T. *ACS Chem. Biol.* **2014**, *9*, 855−866.

(10) Pais, V. F.; Alcaide, M. M.; López-Rodríguez, R.; Collado, D.; Nájera, F.; Pérez-Inestrosa, E.; Álvarez, E.; Lassaletta, J. M.; Fernández, R.; Ros, A.; Pischel, U. *Chem. - Eur. J.* **2015**, *21*, 15369−15376.

(11) Frath, D.; Massue, J.; Ulrich, G.; Ziessel, R. *Angew. Chem., Int. Ed.* **2014**, *53*, 2290−2310.

(12) Frath, D.; Azizi, S.; Ulrich, G.; Retailleau, P.; Ziessel, R. *Org. Lett.* **2011**, *13*, 3414−3417.

(13) Niu, S.-l.; Massif, C.; Ulrich, G.; Renard, P.-Y.; Romieu, A.; Ziessel, R. *Chem. - Eur. J.* **2012**, *18*, 7229−7242.

(14) Frath, D.; Poirel, A.; Ulrich, G.; De Nicola, A.; Ziessel, R. *Chem. Commun.* **2013**, *49*, 4908−4910.

(15) Roubinet, B.; Massif, C.; Moreau, M.; Boschetti, F.; Ulrich, G.; Ziessel, R.; Renard, P.-Y.; Romieu, A. *Chem. - Eur. J.* **2015**, *21*, 14589−14601.

(16) Coskun, A.; Akkaya, E. U. *J. Am. Chem. Soc.* **2006**, *128*, 14474−14475.

(17) Loudet, A.; Burgess, K. *Chem. Rev.* **2007**, *107*, 4891−4932.

(18) Zheng, Q.; Xu, G.; Prasad, P. N. *Chem. - Eur. J.* **2008**, *14*, 5812−5819.

(19) Ulrich, G.; Ziessel, R.; Harriman, A. *Angew. Chem., Int. Ed.* **2008**, *47*, 1184−1201.

(20) Juárez, L. A.; Barba-Bon, A.; Costero, A. M.; Martínez-Máñez, R.; Sancenón, F.; Parra, M.; Gaviña, P.; Terencio, M. C.; Alcaraz, M. J. *Chem. - Eur. J.* **2015**, *21*, 15486−15490.

(21) Juárez, L. A.; Costero, A. M.; Parra, M.; Gil, S.; Sancenón, F.; Martínez-Máñez, R. *Chem. Commun.* **2015**, *51*, 1725−1727.

(22) Lu, H.; Mack, J.; Yang, Y.; Shen, Z. *Chem. Soc. Rev.* **2014**, *43*, 4778−4823.

(23) Rurack, K.; Kollmannsberger, M.; Daub, J. *Angew. Chem., Int. Ed.* **2001**, *40*, 385−387.

(24) Killoran, J.; Allen, L.; Gallagher, J. F.; Gallagher, W. M.; O'Shea, D. F. *Chem. Commun.* **2002**, 1862−1863.

(25) Loudet, A.; Bandichhor, R.; Burgess, K.; Palma, A.; McDonnell, S. O.; Hall, M. J.; O'Shea, D. F. *Org. Lett.* **2008**, *10*, 4771−4774.

(26) Le Guennic, B.; Maury, O.; Jacquemin, D. *Phys. Chem. Chem. Phys.* **2012**, *14*, 157−164.

(27) Koide, Y.; Urano, Y.; Hanaoka, K.; Piao, W.; Kusakabe, M.; Saito, N.; Terai, T.; Okabe, T.; Nagano, T. *J. Am. Chem. Soc.* **2012**, *134*, 5029−5031.

(28) Grimm, J. B.; Sung, A. J.; Legant, W. R.; Hulamm, P.; Matlosz, S. M.; Betzig, E.; Lavis, L. D. *ACS Chem. Biol.* **2013**, *8*, 1303−1310.

(29) Kushida, Y.; Nagano, T.; Hanaoka, K. *Analyst* **2015**, *140*, 685−695.

(30) Yang, Y.; Lowry, M.; Xu, X.; Escobedo, J. O.; Sibrian-Vazquez, M.; Wong, L.; Schowalter, C. M.; Jensen, T. J.; Fronczek, F. R.; Warner, I. M.; Strongin, R. M. *Proc. Natl. Acad. Sci. U. S. A.* **2008**, *105*, 8829−8834.

(31) Stennett, E. M. S.; Ciuba, M. A.; Levitus, M. *Chem. Soc. Rev.* **2014**, *43*, 1057−1075.

(32) Zheng, Q.; Juette, M. F.; Jockusch, S.; Wasserman, M. R.; Zhou, Z.; Altman, R. B.; Blanchard, S. C. *Chem. Soc. Rev.* **2014**, *43*, 1044−1056.

(33) Escobedo, J. O.; Rusin, O.; Lim, S.; Strongin, R. M. *Curr. Opin. Chem. Biol.* **2010**, *14*, 64−70.

(34) Quek, C.-H.; Leong, K. W. *Nanomaterials* **2012**, *2*, 92−112.

(35) Guo, Z.; Park, S.; Yoon, J.; Shin, I. *Chem. Soc. Rev.* **2014**, *43*, 16−29.

(36) Liu, D.; Zhang, Z.; Zhang, H.; Wang, Y. *Chem. Commun.* **2013**, *49*, 10001−10003.

(37) Achelle, S.; Rodríguez-López, J.; Robin-Le Guen, F. *J. Org. Chem.* **2014**, *79*, 7564−7571.

(38) Santos, F. M. F.; Rosa, J. N.; Candeias, N. R.; Carvalho, C. P.; Matos, A. I.; Ventura, A. E.; Florindo, H. F.; Silva, L. C.; Pischel, U.; Gois, P. M. P. *Chem. - Eur. J.* **2016**, *22*, 1631−1637.

(39) Lim, C. W.; Tissot, O.; Mattison, A.; Hooper, M. W.; Brown, J. M.; Cowley, A. R.; Hulmes, D. I.; Blacker, A. J. *Org. Process Res. Dev.* **2003**, *7*, 379−384.

(40) Connolly, D. J.; Lacey, P. M.; McCarthy, M.; Saunders, C. P.; Carroll, A.-M.; Goddard, R.; Guiry, P. J. *J. Org. Chem.* **2004**, *69*, 6572−6589.

(41) Ramírez-López, P.; Ros, A.; Estepa, B.; Fernández, R.; Fiser, B.; Gómez-Bengoa, E.; Lassaletta, J. M. *ACS Catal.* **2016**, *6*, 3955−3964.

(42) Guram, A. S.; Buchwald, S. L. *J. Am. Chem. Soc.* **1994**, *116*, 7901−7902.

(43) Paul, F.; Patt, J.; Hartwig, J. F. *J. Am. Chem. Soc.* **1994**, *116*, 5969−5970.

(44) Ros, A.; Estepa, B.; Ramírez-López, P.; Álvarez, E.; Fernández, R.; Lassaletta, J. M. *J. Am. Chem. Soc.* **2013**, *135*, 15730−15733.

(45) Lippert, E. *Z. Naturforsch., A: Phys. Sci.* **1955**, *10*, 541−545.

(46) Mataga, N.; Kaifu, Y.; Koizumi, M. *Bull. Chem. Soc. Jpn.* **1955**, *28*, 690−691.

(47) Mataga, N.; Kaifu, Y.; Koizumi, M. *Bull. Chem. Soc. Jpn.* **1956**, *29*, 465−470.

(48) Casida, M. E. In *Recent Advances in Density Functional Methods*; Chong, D. P., Ed.; World Scientific: Singapore, 1995; Vol. *1*, p 155−192.

(49) Pais, V. F.; Lassaletta, J. M.; Fernández, R.; El-Sheshtawy, H. S.; Ros, A.; Pischel, U. *Chem. - Eur. J.* **2014**, *20*, 7638−7645.

(50) Greenspan, P.; Fowler, S. D. *J. Lipid Res.* **1985**, *26*, 781−789.

(51) Sackett, D. L.; Wolff, J. *Anal. Biochem.* **1987**, *167*, 228−234.

(52) Belloc, F.; Dumain, P.; Boisseau, M. R.; Jalloustre, C.; Reiffers, J.; Bernard, P.; Lacombe, F. *Cytometry* **1994**, *17*, 59−64.

(53) Gaffield, M. A.; Betz, W. J. *Nat. Protocols* **2007**, *1*, 2916−2921.

(54) Nakamaru, K. *Bull. Chem. Soc. Jpn.* **1982**, *55*, 2697−2705.